

## PLASMA TRANSFER EVENT SEEN BY CLUSTER

Walter J. Heikkilä<sup>(1)</sup>, Patrick Canu<sup>(2)</sup>, Iannis Dandouras<sup>(3)</sup>, Wayne Keith<sup>(4)</sup>, and Yuri Khotyaintsev<sup>(5)</sup>

<sup>(1)</sup>University of Texas at Dallas, Box 830688, Richardson, TX, 75083, USA; heikkila@utdallas.edu

<sup>(2)</sup>CETP/CNRS/UVSQ, 10 Avenue de l'Europe, 78140 Velizy, France; Patrick.Canu@cetp.ipsl.fr

<sup>(3)</sup>Centre d'Etude Spatiale des Rayonnements, 31028 Toulouse, France; Iannis.Dandouras@cesr.fr

<sup>(4)</sup>Angelo State University, ASU Station #10904, San Angelo, TX 76909, USA; wayne.keith@angelo.edu

<sup>(5)</sup>Swedish Institute of Space Physics, Box 537, SE-75121, Uppsala, Sweden; yuri@irfu.se

### ABSTRACT

A plasma transfer event (PTE) was observed by Cluster C3 on 8 March, 2003, beginning at 0707 UT. For over a minute CIS saw, inside the magnetopause, a burst of solar wind plasma with a density up to  $0.8 \text{ cm}^{-3}$ , a factor of 4 higher than was observed before and after. PEACE showed field aligned fluxes at energies up to 500 eV. At higher energies from 1 to 40 keV the fluxes had a pancake distribution indicating closed field lines surrounding the event. The electric field was observed by EFW to vary between -5 and 5 mV/m. WHISPER recorded strong plasma oscillations mostly in two bursts coincident with intense fluxes recorded by PEACE. The other s/c C1, C2, and C4 were in the magnetosheath; the data were used by Sonnerup et al. [32] as evidence for a flux transfer event (FTE), a major question but a separate issue from the PTE.

### 1. Physics of the Magnetopause

The interaction of the solar wind with the dayside magnetopause introduces plasma particles across this boundary. These particles, SW ions and electrons, carry their momentum and energy with them, perhaps modified in the interaction process, into the low latitude boundary layer (LLBL). Two processes were proposed in the same year 1961 for this interaction, magnetic reconnection by Dungey [7] and viscous interaction by Axford and Hines [2]. The first quickly became the preferred explanation as it was apparently able to explain several key features of geomagnetic activity as noted by Sonnerup et al. [31]; this was especially true after the process of a flux transfer event (FTE) was suggested by Russell and Elphic [27] thought to be time-dependent reconnection. The second, viscous interaction, is a result of the massive tailward plasma flow in the low latitude boundary layer (LLBL), suggested by Cole also in 1961 [5], discovered later by Hones et al. [14]. The concept of a plasma transfer event [13, 19] is essential for the efficient transport of SW plasma across the magnetopause into the LLBL on closed field lines.

The Cluster quartet of spacecraft witnessed an event on March 8, 2003 after 0707 UT that is highly relevant to this important question. That was discussed in the recent article "Anatomy of a flux transfer event

seen by Cluster" by Sonnerup et al. [2004]. We present data analysis of a plasma transfer event (PTE) on C3 for the same event.

### 2. Anatomy of a Flux Transfer Event (FTE)

Fig 1 displays some relevant data from all s/c for 20 m; the region marked FTE2 from 0707-0709 was discussed in Sonnerup et al. [32], also here but only C3. Their paper is an example of superb usage of the Cluster data for one event, as shown dramatically by their Figure 2. The FTE was observed near the northern cusp; the GSE location was approximately (7.1, 2.5, 7.4)  $R_E$  with the spacecraft separations being about 5000 km.

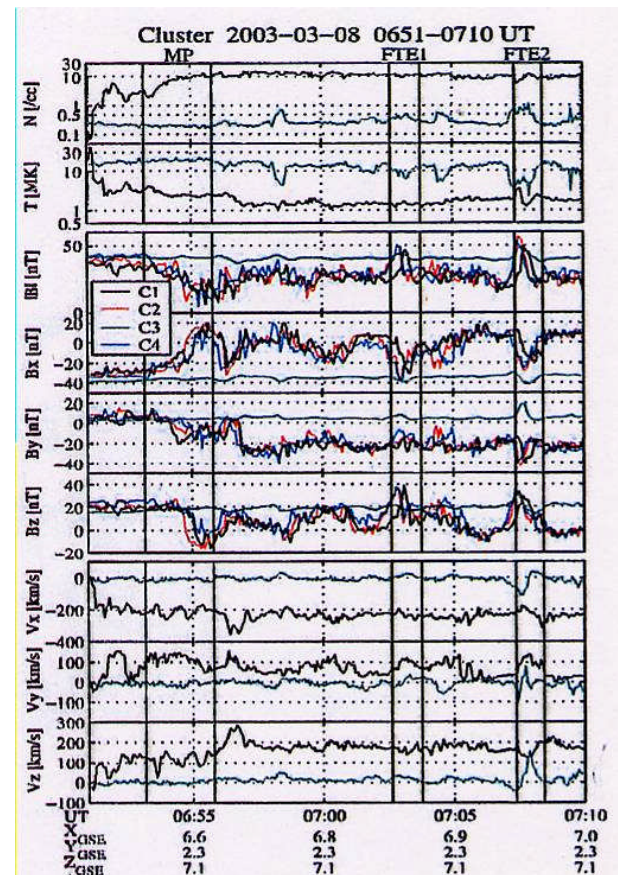


Fig. 1. Records of C1, C2, C4 from the magnetosphere, MP, and two flux transfer events. C3 was in the magnetosphere throughout; C3 at FTE2 is treated here.

Data from Cluster (all 4 spacecraft) were used to study the structure of the FTE. Immediately before and after the event C3 was located mainly in the magnetosphere whereas the other three spacecraft were measuring magnetosheath-like conditions. In the event itself, all spacecraft recorded a pronounced maximum in field magnitude. A peak in number density accompanied by a minimum in temperature was seen by C3.

The speed of the structure relative to the spacecraft was determined as the deHoffmann-Teller (HT) frame velocity. The frame velocity  $V_{HT}$  relative to the spacecraft was obtained from a least squares procedure. In this frame the plasma flow is as nearly field aligned as the velocities and magnetic fields, measured during the event, permit. The proper frame of the FTE structure slides along the magnetopause past the observing spacecraft. Additionally, it shares the inward/outward motion of the magnetopause. They find that the velocity revealed by Cluster is well anchored to the HT high speed flow at (-234, 51, 166) km/s, anti-sunward, duskward and poleward. The flux rope has a strong core field “which must have been created by component merging at some site equatorward of Cluster. ... The absence of reconnection signatures implies that, by the time the FTE reaches Cluster, it is nearly a fossil structure.” They suggest that the average reconnection electric field for this FTE must have been at least as large as 0.18 mV/m.

### 3. Observations of a Plasma Transfer Event (PTE)

In the limited amount of space in this preliminary report we show only data in the next 4 figures.

#### 3.1 CIS ion data

Figure 2 displays the ion data obtained by the CIS experiment as described by Rème et al. [27], obtained onboard spacecraft C3 between 07:07 and 07:09 UT. The top five panels give the energy-time ion spectrograms from the HIA sensor (no mass discrimination), for ions arriving in the  $90^\circ \times 180^\circ$  sector with a field-of-view pointing in the sun, dusk, tail, and dawn direction respectively, and then the omnidirectional ion flux. The following four panels show the omnidirectional ion flux measured by the CODIF sensor, separately for  $H^+$ ,  $He^{++}$ ,  $He^+$  and  $O^+$  ions. All spectrogram units are in particle energy flux ( $keV cm^{-2} s^{-1} sr^{-1} keV^{-1}$ ). The density values are given in the bottom two panels, for the HIA sensor (no mass discrimination) and the CODIF sensor (separately for  $H^+$ ,  $He^{++}$ ,  $He^+$  and  $O^+$  ions). The PTE associated burst of plasma is clearly seen in the data. The density, during the event, increases by a factor of 4, and the presence of  $He^{++}$  ions confirms its solar wind origin.

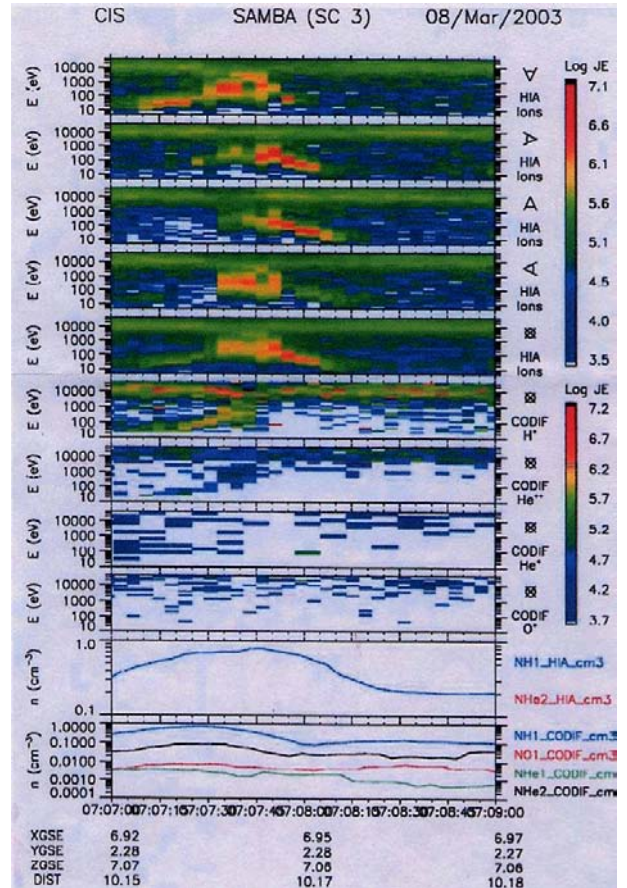


Fig. 2: C3 observed a burst of SW plasma for over 1 minute. The first 4 show the spectrograms in different directions. Observation of  $He^{++}$  confirms it's identity as the solar wind. The increase in density is up to a factor of 4.

#### 3.2 PEACE electron data

Electron measurements were obtained by the Plasma Electron And Current Experiment. PEACE consists of two sensors with hemispherical electrostatic analyzers, each with a  $180^\circ$  field of view radially outwards and perpendicular to the spin plane. Together, the sensors cover an energy range from 0.6 eV up to 26 keV over twelve polar sectors after Johnstone et al. [15]. The data shown were taken by the High Energy Electron Analyzer (HEEA) sensor on Cluster-3, covering the energy range from 34 eV to 22 keV. Pitch angle distributions were determined on-board at one spin resolution. Thirteen pitch-angle bins and 30 energy steps are telemetered in this mode, which were reduced to the 10 energy bins shown in Figure 3. Full-resolution pitch-angle data is retained within each energy bin, going from 0 degrees at the top of each panel to  $180^\circ$  degrees at the bottom. The bottom panel labeled “Flow AZ” shows the spin angle traveled between the start of the spin and the sensor aperture facing the magnetic field direction.

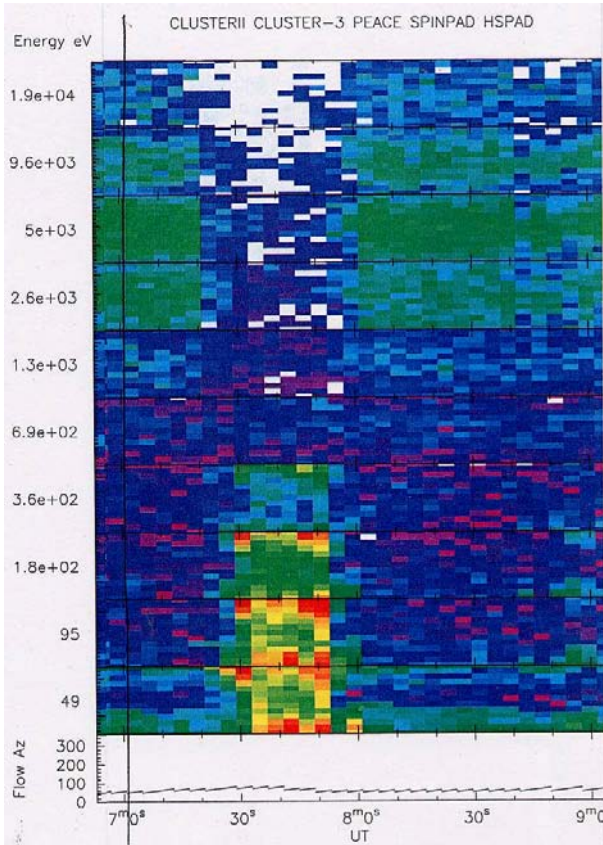


Fig. 3. PEACE electron data divided into 10 channels with the center energy indicated on the left. Each channel is divided into pitch angle with  $0^\circ$  at the top,  $180^\circ$  at the bottom. The electron counting rate at the highest energies maximizes near  $90^\circ$ , indicating trapping on closed field lines surrounding the event. At lower energies the data show intense electron bursts in the PTE.

### 3.3 WHISPER plasma emissions

Figure 4 illustrates the emissions observed up to 40 kHz by WHISPER [Pickett et al., 26] on the four spacecraft during the FTE2 event identified in Figure 1. The differences in the signatures observed between C1, C2, C4, in the magnetosheath and C3 in the magnetosphere are evident. The faint emissions close to 30-35 kHz is the local plasma frequency, corresponding to a local density of  $\sim 10$ -15 e/cc for C1, C2, C4. The bursty broadband emissions observed at low frequencies are also common in this region and due to solitary potential structures [23]. In the magnetosphere, C3 is detecting a lower density plasma, identified here by the low frequency cut-off of the continuum radiation at 8 kHz ( $N_e \sim 0.8$  e/cc). The signatures associated with the boundary of the PTE are very strong bursts, up to  $\sim 1$  mV/m, of upper hybrid emissions, which are probably triggered by the low energy field aligned beams observed by the PEACE instruments (see figure 3). Intense broadband emissions, more than two orders of magnitude above background, possibly triggered by the counterstreaming electron beams reported from Peace data are observed when C3 penetrates the PTE.

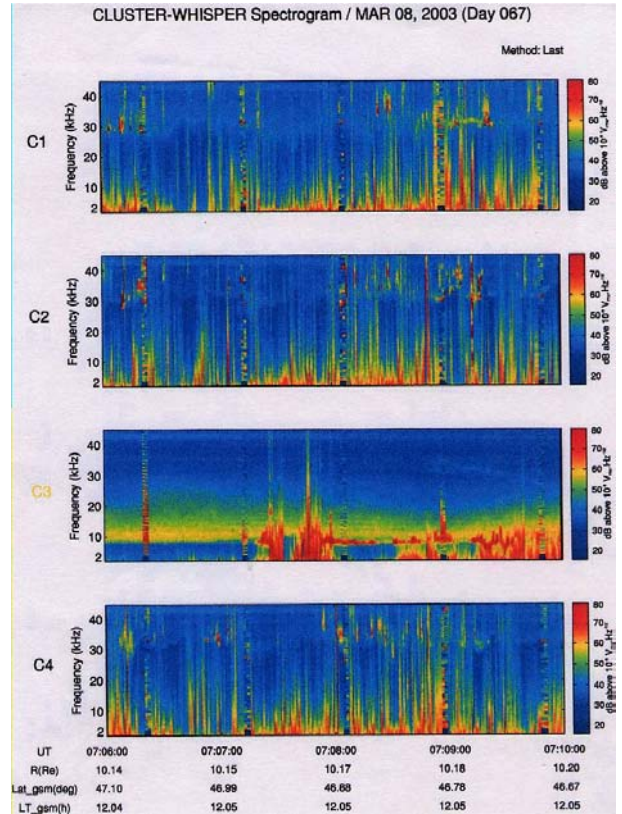


Fig. 4. Plasma emissions from C1, C2, and C4 are quite different from those observed by C3. The latter shows intense bands on either side of the PTE.

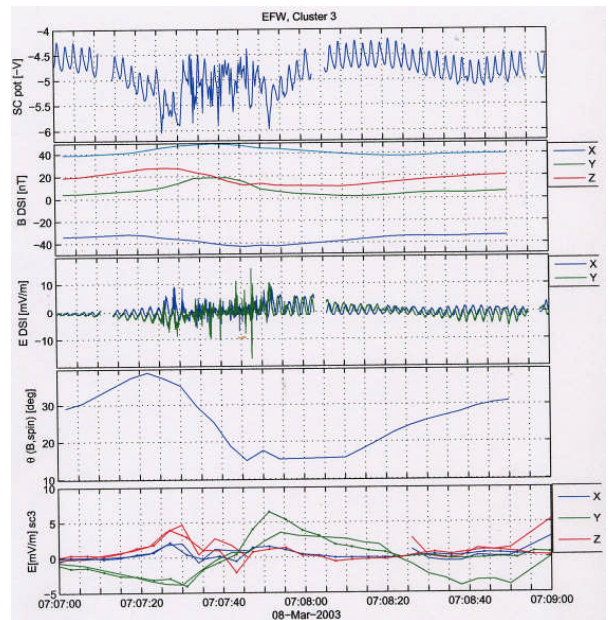


Fig. 5. Panels from top to bottom show: negative of the spacecraft potential, magnetic field, high resolution electric field from one boom pair, angle between the spacecraft spin plane and the magnetic field, spin resolution electric field (the z-component electric field is calculated assuming  $\mathbf{E} \cdot \mathbf{B} = 0$ , the dash-dot lines are components of  $\mathbf{V} \times \mathbf{B}$  from CIS HIA).

### 3.4 EFW data

Figure 5 presents electric field measurements during the interval 07:07--07:09 UT after Gustafsson et al. [9]. The upper panel shows negative of the spacecraft potential which indicates a density/temperature change around 07:07:10--07:08:00. Middle panel shows a simultaneous enhancement of wave activity in a frequency range between 0.25 to 10 Hz. One should note that the electric field presented is coming from only one probe pair, and thus represents an incomplete measurement of the electric field. The last panel shows spin resolution electric field measured by the EFW and CIS HIA. One can see a clear bipolar signature in  $E_y$  between 07:07:10 and 07:08:00, where  $E_y$  is changing from negative to positive in the middle of the structure at 07:07:40 UT.

## 4. The concept of a plasma transfer event

There is no question about the reality of a plasma transfer event (PTE); observations come from a variety of sources beginning with the rocket results of Carlson and Torbert [4] (see the reviews by Lundin [19], Lemaire and Roth [16, 17], Heikkila [13], and Lundin et al. [20]). The concept of PTE is not as well known as the FTE so we describe it here, however briefly.

It is very important that we pay close attention to the reference frame; we use 2 frames called the laboratory frame and the reconnection frame. Conservation of momentum and energy of the entire system is the goal. Maxwell's equations are an expression of Helmholtz's theorem for the two fields  $\mathbf{E}$  and  $\mathbf{B}$ . Poynting's Theorem (obtained directly from Maxwell's equations) allows one to see essential differences between the various processes on the interaction of solar wind plasma at the magnetopause:

$$\iiint_{vol} \mathbf{E} \cdot \mathbf{J} d\tau = -\frac{1}{\mu_0} \oint_{surf} \mathbf{E} \times \mathbf{B} \cdot d\mathbf{S} \quad (1)$$

$$-\frac{\partial}{\partial t} \iiint_{vol} \left( \frac{\epsilon_0 E^2}{2} + \frac{B^2}{2\mu_0} \right) d\tau \quad (2)$$

This is a cause and effect relationship regarding energy. The cause (source of energy, a dynamo with  $\mathbf{E} \cdot \mathbf{J} < 0$ , terms on the right) indicates that the plasma yields its energy to the electromagnetic field; the effect (dissipation with  $\mathbf{E} \cdot \mathbf{J} > 0$ , term to the left) is the electrical load. In either case, a source of energy is required ( $\mathbf{E} \cdot \mathbf{J} < 0$ ), in the *same* current circuit, to provide for the reconnection load ( $\mathbf{E} \cdot \mathbf{J} > 0$ ).

In the case of magnetic reconnection (eq. 1), Poynting flux originates from some external source, a dynamo somewhere else in the current circuit. Equivalently, a Poynting flux carries this energy, but this too comes from this dynamo [13]. The Dungey model of the magnetosphere has a dynamo with  $\mathbf{E} \cdot \mathbf{J} < 0$  over the lobe magnetopause by Cowley [6]; it is not clear where the dynamo for the FTE is located.

Three dimensions are required for a realistic considering of local effects (eq. 2). The relevant terms occur only in the volume integrals of Poynting's theorem, expressing changes in electric and magnetic energy densities. Because of time limitations energy cannot travel super-Alfvénically; the relevant volume must be closely confined. This is quite different from the steady state. There are two complementary processes: (1) the polarization electric field, which does not depend on the movement of the magnetopause itself, and (2) the inductive electric field due to magnetopause erosion, which does.

Lemaire and Roth [16, 17] used electric energy of the plasma, i.e. plasma in motion, in a process they called *impulsive penetration* (IP). This was based on the pioneering work by Schmidt [29, 30], and the results of laboratory experiments by Baker and Hammel [3].

Heikkila [11, 12] used a different process, that of tapping magnetic energy with the induction electric field; he used the term plasma transfer event (PTE) after Carlson and Torbert [4], Lundin and Evans [18], Woch and Lundin [33]. The changing  $\delta\mathbf{B}$  due to a perturbation current  $\delta\mathbf{J}$  is *a change in the state of interconnection* (the obvious term *magnetic reconnection* is reserved for the very different process suggested by Dungey [7], Owen and Cowley [22], Sonnerup et al., [32] and many others).

There is also polarization of the plasma in a PTE. Both processes (IP and PTE) play key roles [13]; tapping both electric and magnetic energy is involved in getting SW plasma through the MP.

### 4.1 Fundamentals

To begin at the beginning, we note that the electric field has 2 sources, charge separation and induction. For this reason it is better to use the E,J paradigm rather than the B,V discussed by Parker [23]; with the B,V there is only one electric field, the convection electric field:

$$\mathbf{E} = -\mathbf{V} \times \mathbf{B} + \text{other terms} \quad (3)$$

The only source of a magnetic field is a current  $\mathbf{J}$  by Ampere's law; therefore, to study changes in the magnetic field we should consider perturbation electric currents  $\delta\mathbf{J}$ , the source of  $\delta\mathbf{B}$ . A changing current will create an induction electric field, by Lenz's law. We focus on the electric field directly, noting that the total field  $\mathbf{E}$  is

$$\mathbf{E} = \mathbf{E}^{es} + \mathbf{E}^{ind} = -\nabla\phi - \partial\mathbf{A} / \partial t \quad (4)$$

has both the electrostatic and induction components. The plasma response to the imposition of the induced electric field  $\mathbf{E}^{ind} = -\partial\mathbf{A} / \partial t$  leads to the creation of an electrostatic field  $\mathbf{E}^{es} = -\nabla\phi$ , at least when conductivities are not zero.

A PTE is three-dimensional object, 2-D to show the magnetic topology ( $x$ - $z$  plane in GSM coordinates), and another set to show localization involving curl  $\mathbf{E}$  ( $x$ - $y$  plane). These two types of field have different topological characteristics, one being solenoidal with  $\nabla \cdot \mathbf{E}^{ind} = 0$  using the Coulomb gauge discussed extensively by Morse and Feshbach [21], the other being irrotational (conservative) with zero curl,  $\nabla \times \mathbf{E}^{es} = 0$ . Consequently, they can *never cancel each other*; the most the plasma can do is to redistribute the field while maintaining the curl.

It is instructive to express the induction electric field in integral form:

$$emf = \varepsilon = \oint_{\text{circuit}} \mathbf{E} \cdot d\mathbf{l} = -d\Phi^{mag} / dt \quad (5)$$

where  $\Phi^{mag}$  is the magnetic flux through the circuit used for the integration. It is only by this emf that we can tap stored magnetic energy.

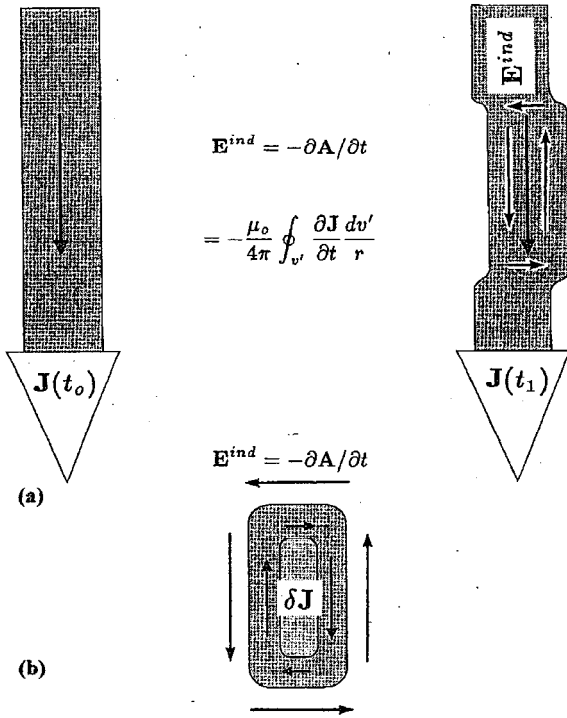


Fig. 6. (a) The unperturbed magnetopause current is shown on left; this is the frame used in reconnection theories where the reconnection electric field is shown embedded (supposedly due to anomalous resistivity along the X-line in the magnetic field topology in the normal plane). PTE assumes a different approach, that of a localized meander of the MP current on the right. This is associated with an induction electric in the frame of the unperturbed MP current. (b) The perturbation current by itself.

#### 4.2 Localized pressure pulse

The inferred immediate cause of a plasma transfer event is a localized pressure pulse from the magnetosheath, an inward push by solar wind plasma associated with erosion found by Aubry et al. [1]. The pressure pulse is

likely to be in some small region, not extending to infinity in the  $y$ -direction (Fig. 6).

Only the induction electric field is shown in Fig. 6; the plasma response through charge separation (creating an electrostatic field) is treated in next three subsections. On the left is the undisturbed magnetopause current  $\mathbf{J}(t_0)$  before the pressure pulse; on the right is the condition after the first strike (the tangential velocity is assumed to vanish here; its effect will be discussed in Fig. 9). The total current perturbation  $\delta\mathbf{J}$  is shown in Figure 6 at the bottom; it is this change in current which induces a voltage (by Lenz's law):

$$\mathbf{E}^{ind} = -\frac{\partial \mathbf{A}}{\partial t} = -\frac{\mu_0}{4\pi} \iiint_{\tau} \frac{\delta \mathbf{J}}{r} d\tau \quad (6)$$

where  $\mathbf{A}$  is expanded to show the dependence on the time rate of the current. The field is in the reference frame of the undisturbed current on the left, the laboratory frame, everywhere opposing the perturbation (note the negative sign). This induction electric field causes the earthward flow of both magnetosheath and magnetospheric plasma in step with the moving magnetopause.

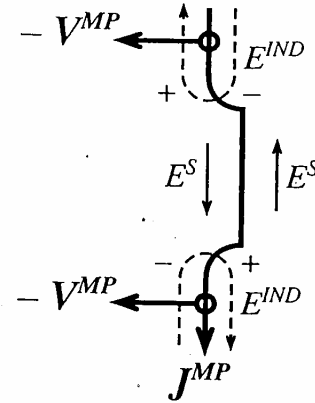


Fig. 7. In this view it is assumed that the frame of reference is fixed to the magnetopause in the center, as in reconnection models. The magnetopause is moving sunward, top and bottom in view of the localized perturbation. If there is a normal component of the magnetic field through the current sheet  $E^{ind}$  can polarize the plasma, causing an electrostatic field tangential to the MP, reversing as indicated. We see that this  $E^{es}$  will drive the SW plasma into the current sheet.

#### 4.3 Motion of the magnetopause

A localized induction electric field,  $\mathbf{E}^{ind} = -\partial \mathbf{A} / \partial t$ , is forced upon the plasma, not an electrostatic field. It is entirely local, opposed to the current perturbation. This solenoidal feature is consistent with the inward motion of the magnetopause as in Fig. 7. Here it is assumed that the frame of reference is fixed to the magnetopause in the center, as in reconnection models.

Let's assume that the perturbation is very wide so that the electric field  $E^{es}$  shown becomes quite small and can be neglected. The induction has a tangential component at each side the perturbation, which reverses as in Fig. 6, so the plasma on both sides of the MP is moving to the left, in step with the MP.

Now let's bring in a narrower perturbation as shown in Fig. 7. With a *localized perturbation* the magnetopause at the top and bottom is moving sunward in our frame of reference; now the induction electric field is here. It has a component normal to the magnetopause at the edges of the perturbation, with opposite polarities. We need to consider 2 cases regarding  $B_n$ .

If  $B_n = 0$  the plasma cannot respond by charge separation as shown by + and - signs, no electrostatic field is created;  $E^{es}$  is zero. It should be noted that the induction has a normal component at each side the perturbation, which reverses as in Fig. 6, and we recover the previous case.

However, if there is a normal component of the magnetic field through the current sheet  $E^{ind}$  can polarize the plasma along  $B_n$  causing an electrostatic field tangential to the MP, reversing as indicated. We see that this  $E^{es}$  will drive the SW plasma into the current sheet, in the reconnection frame. This is contrary to the views of Owen and Cowley [22].

#### 4.4 Response of the plasma: $B_n = 0$

To return to the laboratory frame Fig. 6, the electric field shown is not the actual electric field observed on a satellite, or even in the magnetopause frame (the reconnection frame). The plasma response is hindered by the magnetic field if  $B_n$  vanishes. Because  $B_z$  is the dominant component of the magnetic field on either side of the magnetopause (at least for high as well as low shears), the very low Pedersen conductivity  $\sigma_1 \sim 0$  for a collisionless plasma in the tangential  $y$  direction limits polarization of charge in that direction. The induction electric field alone is the field that determines the motion of the plasma over the bumpy surface, a velocity that is everywhere tangential to the local magnetopause [24, 25].

#### 4.5 Response of the plasma: $B_n$ is finite

The plasma response changes dramatically with an open magnetosphere. In this case, a rotational discontinuity will be present, with a finite  $B_n$ . Electron and ion mobilities are high along the magnetic field. Now we can use the very large direct conductivity  $\sigma_0$ ; the plasma can polarize along the magnetic field lines as shown in Figure 7, top and bottom, in *different senses*, causing an electrostatic field tangential to the MP, reversing as indicated. Thus we see that this  $E^{es}$  will drive the SW plasma into the current sheet. On the other side, since both  $B$  and  $E$  reverse, the electric drift  $\mathbf{E} \times \mathbf{B}$  will be also earthward. A PTE is produced.

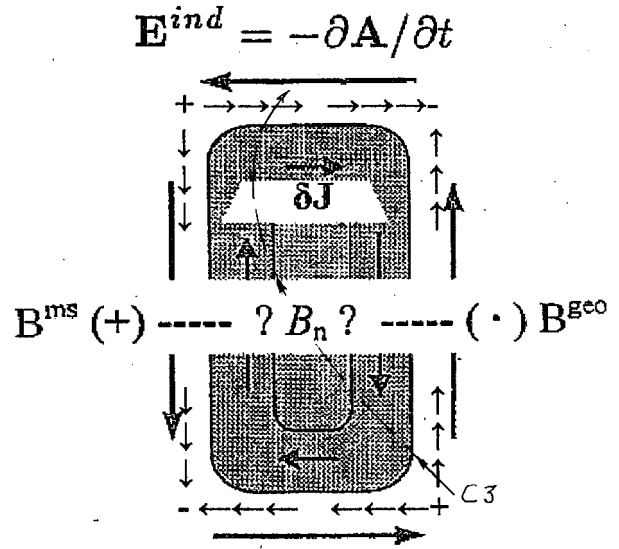


Fig. 8. If  $B_n$  is finite, then plasma can polarize in response to the induction electric field. Any reduction in the net  $E_{||}$  (top and bottom) in an arbitrary closed contour involves enhancement of the perpendicular component at least somewhere around the chosen contour, otherwise the curl (emf) would be affected. The tangential component of the induction field will be enhanced by the plasma.

This is elaborated further by Fig. 8, Fig. 6(b) but showing the plasma response by creating an electrostatic field. Because it has no curl, an electrostatic field can have no effect on the curl, or electromotive force, of the induction field. Any reduction in the net  $E_{||}$  in an arbitrary closed contour involves enhancement of the perpendicular component at least somewhere around the chosen contour, otherwise the curl (emf) would be affected. Whatever the distribution of the secondary field  $E_{||}^{es}$ , the resultant field has to remain finite and large enough to make the line integral finite and equal to  $-d\Phi^M/dt$  by eq. 6 [12]. The result of a cancellation, or even a partial cancellation, is a tangential (to the MP) electrostatic field  $E_p^{es}$  directed oppositely on the two sides of the localized current meander, enhancing the induction component. In the frame of the moving MP this extra  $E_{\perp}$  ( $= E_{tan}$  to MP) will cause a finite  $V_n$  through the MP, exactly as found in the high shear case of Phan et al. [24], and Phan and Paschmann [25]. A finite  $B_n$  is crucial to the analysis of a PTE. (see Figure 8)

#### 4.6 Tangential motion

It is essential to include the tangential motion (to the magnetopause) to understand the effects of a PTE upon the physics of the magnetosphere. In the magnetosheath all the SW plasma is moving anti-sunward, even super-Alfvénically toward the flanks. Whatever plasma penetrates through the MP must face conditions in a new medium. The two black arrows are meant to denote the tailward motion of the plasma, higher in the MS, lower in the low latitude boundary layer (LLBL). For

example, this difference makes it possible to have multiple injection events in the LLBL due to successive blasts from the magnetosheath as observed by Carlson and Torbert [4] and Woch and Lundin [33].

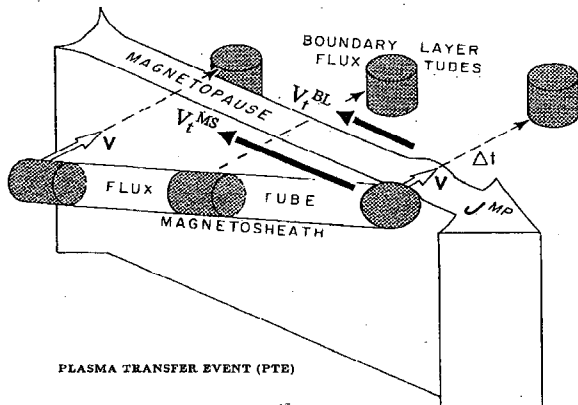


Fig. 9. In the magnetosheath all the SW plasma is moving anti-sunward, even super-Alfvénically toward the flanks. Whatever plasma penetrates through the MP must face conditions in a new medium. The two black arrows are meant to denote the tailward motion of the plasma, higher in the MS, lower in the low latitude boundary layer (LLBL).

## 5. A plasma transfer event seen by Cluster

This process was seen by C3 as shown by Fig. 2. CIS/CODIF data showing penetration of solar wind plasma lasting for over 1 minute at the time of the event just described. The presence of  $\text{He}^{++}$ , and the similar shape of  $\text{H}^+$  profile, verifies this identification of SW plasma. The plasma density is increased, quadrupled in the middle, for over one minute, in a burst of plasma entering through the magnetopause.

PEACE electron data show several aspects in agreement with a PTE. (1) The pitch angle distribution for the higher energy channels has a maximum near  $90^\circ$ , indicating field lines are closed on either side. (2) In the heart of the PTE these fluxes are greatly reduced but still showing some maximum at  $90^\circ$ . Since  $B_n$  is small compared to the magnetic field on the either side (magnetosheath and LLBL) their will be some trapping along  $B_n$  in the current layer. This result may indicate open magnetic field lines, a firm requirement for the PTE process. (3) At lower energies intense fluxes are observed, with a maximum at  $0^\circ$  at 0730 and  $180^\circ$  at 0742. Taking note of the speed of the disturbance [32], this is consistent with a vertical dimension in Fig. 8 of 3,500 km ( $0.5 R_E$ ) for  $\delta J$ .

WHISPER instrument showed two bursts of plasma emissions at the beginning and end of the PTE. It is likely that these bursts coincided with parallel component of the induction electric field as shown in Fig. 8. These bursts probably produced the emissions.

EFW instrument also showed the bursty structure. The DC electric field showed that the sense reversed in  $E^y$ ; it was strong in magnitude ( $\sim 5$  v/km). Fig. 8 includes a possible trajectory of C3 through the PTE.

## 6. Discussion

After many years of research on the interaction process of solar wind plasma at the magnetopause the big question is still the details of the processes involved. There are two problems that we need to confront.

### 6.1 Diversion of the magnetosheath flow

The diversion of the magnetosheath flow around the magnetospheric obstacle (the magnetopause) involves more than 90% of the solar wind intercepted by the bow shock, about  $10^{28}$  ions/s. This is a major problem that Sonnerup et al. [32] have faced.

However, they should not have included C3 in their analysis. With C3 left out they would be released from at least three difficulties.

- The fit would be better; as they said, “This relatively low value [of the correlation coefficient] is a consequence of the fact that C1 and C3 separately gave somewhat different  $\mathbf{V}_{HT}$  vectors”;
- The velocities for C3 were supersonic, violating the conditions of their analysis;
- The temperature minimum on C3 at FTE2 is quite visible in Fig. 1. The reconnection process requires dissipation with  $\mathbf{E} \cdot \mathbf{J} > 0$ , implying a temperature maximum.

### 6.2 Penetration of some SW plasma into the LLBL

The temperature minimum follows from the action of the dynamo, with  $\mathbf{E} \cdot \mathbf{J} < 0$  on the right in Fig. 8; the plasma is *losing*, not gaining, energy [12]. This process is supported by the electric field observations in Fig. 5:  $E_y$  reverses as opposed to being constant as assumed in the reconnection model.

Some SW plasma (less than 10%) does penetrate through the magnetopause into the magnetosphere (LLBL), about  $10^{27}$  ions/s deduced by Eastman [7]. This does happen quickly, in a few seconds with individual events.

The PTE is a likely candidate. The electrostatic field  $E^{es}$  (Fig. 7) will drive the SW plasma into the current sheet. On the other side, since both  $\mathbf{B}$  and  $\mathbf{E}$  reverse, the electric drift  $\mathbf{E} \times \mathbf{B}$  will be also tailward. Particles go wherever the local electric and magnetic fields direct them; they have no time to check whether they are on open  $\mathbf{B}$  or not. From open field lines in the MP current sheet the particles go to closed field lines in the low latitude boundary layer.

Another order of magnitude (or even more) is involved for the plasma source of the plasma sheet,  $10^{26}$  to  $10^{25}$  ions/s. This minute fraction,  $10^{-2}$  to  $10^{-3}$ , is responsible for all the glorious auroral displays!

### Acknowledgment

It is a pleasure to work with Cluster, and the Cluster team! (WJH).

## 7. References

- [1] Aubry, M. P., et al., Inward motion of the magnetopause before a substorm, *J. Geophys. Res.* **75**, 7018, 1970.
- [2] Axford, W. I. and C. O. Hines, A unifying theory of high-latitude geophysical phenomena and geomagnetic storms, *Can. J. Phys.*, **39**, 1433, 1961.
- [3] Baker, D. A. and J. E. Hamell, Experimental Studies of the Penetration of Plasma Stream into a Transverse Magnetic Field, *Phys. of Fluids*, **8**, 713, April 1965.
- [4] Carlson, C. W., and R. B. Torbert, Solar Wind Ion Injections in the Morning Auroral Oval, *J. Geophys. Res.*, **85**, 2903, 1980.
- [5] Cole, K. D., On solar wind generation of polar geomagnetic disturbances, *Geophys. J. Roy. Astro. Soc.* **6**, 103, 1961.
- [6] Cowley, S. W. H., Plasma populations in a simple open model magnetosphere, *Space Sci. Rev.*, **26**, 217, 1980.
- [7] Dungey, J. W., Interplanetary magnetic field and the auroral zones, *Phys. Rev. Lett.*, **6**, 47, 1961.
- [8] Eastman, T. E., *The Plasma Boundary Layer and Magnetopause Layer of the Earth's Magnetosphere*, Ph. D. Thesis, University of Alaska, 1979.
- [9] Gustafsson, G., et al., The electric Field and Wave Experiment for the Cluster Mission, *Space Science Reviews*, **79**(1 - 2), 137 - 156, 1997.
- [10] Heikkila, W. J., et al., Potential and Induction Electric Fields in the Magnetosphere During Auroras, *Planet. Space Sci.*, **27**, 1383, 1979.
- [11] Heikkila, W. J., Impulsive plasma transport through the magnetopause, *Geophys. Res. Lett.* **9**, 159, 1982.
- [12] Heikkila, W. J., Interpretation of Recent APMTE Data at the MP, *J. Geophys. Res.*, **102**, 2115, 1997.
- [13] Heikkila, W. J., Cause and effect at the magnetopause, *Space Sci. Rev.* **83**, 373, 1998.
- [14] Hones, E. W., Jr., et al., Measurements of magnetotail plasma flow made with Vela 4B, *J. Geophys. Res.*, **77**, 5503, 1972.
- [15] Johnstone, A. D., et al., PEACE: A Plasma Electron and Current Experiment, *Space Sci. Rev.*, **79**, 351, 1997.
- [16] Lemaire, J. and M. Roth, Penetration of solar wind plasma elements into the magnetosphere, *J. Atmos. Terr. Phys.*, **40**, 337, 1978.
- [17] Lemaire, J. and M. Roth, Non-steady-state solar wind-magnetosphere interaction, *Space Sci. Rev.*, **57**, 59, 1991.
- [18] Lundin, R. and D. Evans, Boundary layer plasmas as a source for high-latitude, early afternoon, auroral arcs, *Planet. Space Sci.*, **33**, 1389, 1985.
- [19] Lundin, R., On the Magnetospheric Boundary Layer and Solar Wind Energy Transfer into the Magnetosphere, *Space Sci. Rev.*, **48**, 263, 1988.
- [20] Lundin, R.; et al., Evidence for impulsive solar wind plasma penetration through the dayside magnetopause, *Ann. Geophys.*, **21**, 457, 2003.
- [21] Morse, P. M. and H. Feshbach, *Methods of Theoretical Physics*, McGraw Hill, 1953.
- [22] Owen, C. J., and S. W. H. Cowley, Heikkila's mechanism for impulsive plasma transport through the magnetopause: A re-examination, *J. Geophys. Res.* **96**, 5565, 1991.
- [23] Parker, E. N., The alternative paradigm for magnetospheric physics, *J. Geophys. Res.*, **10**, 10.587, 1996.
- [24] Phan, T.-D., et al., The magnetosheath region adjacent to the dayside magnetopause: AMPTE/IRM observations, *J. Geophys. Res.* **99**, 121, 1994.
- [25] Phan, T.-D and Götz Paschmann, The low-latitude dayside magnetopause and boundary layer for high magnetic shear: Structure and motion, *J. Geophys. Res.* **101**, 7801, 1996.
- [26] J. S. Pickett, et al., Solitary Potential Structures Observed in the Magnetosheath by the Cluster Spacecraft, *Nonlinear Processes in Geophys.*, **10**, pp. 3-11, March 11, 2003.
- [27] Rème H., et al., First multispacecraft ion measurements in and near the Earth's magnetosphere with the identical Cluster ion spectrometry (CIS) experiment, *Ann. Geophys.*, Vol. **19**, 1303, 2001.
- [28] Russell, C. T. and Elphic, R. C., Initial ISEE magnetometer results: Magnetopause observations, *Space Sci. Rev.*, **22**, 681, 1978.
- [29] Schmidt, G., Plasma motion across magnetic fields, *Phys. Fluids*, **3**, 961, 1960.
- [30] Schmidt, G., *Physics of High Temperature Plasmas*, Academic Press, 1979.
- [31] Sonnerup et al., Fluid Aspects of Reconnection at the Magnetopause: In Situ Observations, in *Physics of the Magnetopause*, AGU Monograph **90**, 167, 1995.
- [32] Sonnerup, B., U. Ö., et al., Anatomy of a flux transfer event seen by Cluster, *Geophys. Res Lett*, **31**, June 2004.
- [33] Woch, J. and R. Lundin, Signatures of transient undary layer processes observed with Viking, *J. Geophys. Res.* **97**, 1431, 1992.